Quaternary Research 57, 49–57 (2002)
doi:10.1006/qres.2001.2289, available online at http://www.idealibrary.com on IDEAL®

Sediment-Color Record from the Northeast Atlantic Reveals Patterns of Millennial-Scale Climate Variability during the Past 500,000 Years

Jan P. Helmke[1]

GEOMAR Research Center for Marine Geosciences, Wischhofstr. 1-3, D-24148 Kiel, Germany

Michael Schulz

Institute for Geosciences, University of Kiel, Olshausenstrasse 40, D-24118 Kiel, Germany

and

Henning A. Bauch

Alfred-Wegener Institute for Polar and Marine Research, Columbusstrasse, D-27568 Bremerhaven, Germany

Received April 30, 2001

A 500,000-yr-long deep-sea sediment-color record from the Northeast Atlantic was investigated to reconstruct the evolution of late Pleistocene climate variability on millennial time scales. Variations of the red–green color intensity are probably caused by climatically induced changes in the ice-rafted input of red-colored iron-bearing terrigenous material to the core site. The resolution of the age model impedes the detection of distinct spectral features at sub-Milankovitch periodicities. Hence, millennial-scale climate variability is quantified as time-dependent variance of the high-pass filtered color time series. The course of the estimated variance shows distinct patterns, which can be linked to continental ice mass. During the past 500,000 yr, large-amplitude millennial-scale climate variability occurs only if continental ice mass exceeds a threshold level, equivalent to sea level at approximately 40% of the lowering during the last glacial maximum.

Key Words: **sediment color; Northeast Atlantic; glacial–interglacial climate; millennial-scale variability; threshold level.**

INTRODUCTION

Climate proxy data from various archives document large-amplitude climate fluctuations during the last glacial period on millennial time scales, i.e., variability between 10^3 and $<10^4$ yr. On longer time scales these include Heinrich events (e.g., Bond *et al*., 1992) with an average recurrence time of approximately 7000 yr (Sarnthein *et al*., 2001) and on shorter scales Dansgaard-Oeschger events (Dansgaard *et al*., 1993; Grootes and Stuiver, 1997) with a spacing of approximately 1500 yr and multiples thereof (Alley *et al*., 2001; Schulz, in press). Heinrich events are thought to be linked to internal oscillations of the Laurentide ice sheet (MacAyeal, 1993), whereas the origin of the Dansgaard–Oeschger events remains controversial, ranging from internal oscillations of the ocean–atmosphere system (Broecker *et al*., 1990; Winton, 1993; Sakai and Peltier, 1997) to periodic calving of the Greenland ice sheet (van Kreveld *et al*., 2000) and to external forcing mechanisms (van Geel *et al*., 1999; Keeling and Whorf, 2000). Furthermore, it has been suggested that millennial-scale climate variability, although with smaller amplitude, is not restricted to the last glacial period but is a pervasive feature of the recent interglaciation, the Holocene (Bond *et al*., 1997; deMenocal *et al*., 2000).

The possible interference of anthropogenic climate perturbations with natural climate fluctuations on millennial time scales is a challenging task in predicting future climate change. Previous studies demonstrated the suitability of color records from marine sediments to quantify millennial-scale climate change with high temporal resolution (Cortijo *et al*., 1995; Ortiz *et al*., 1999). However, marine sediment color records have so far not been used to document the evolution of millennial-scale climate fluctuations throughout the Late Quaternary. To gain better insight into these natural variations we analyze a high-resolution color record from Northeast Atlantic deep-sea sediments, which documents climate variability down to millennial time scales over the last five glacial–interglacial cycles.

DATA AND STRATIGRAPHY

Core M23414 was taken at the Rockall Plateau in the Northeast Atlantic (Fig. 1) on the northeastern fringe of Ruddiman's North Atlantic ice-rafted debris (IRD) belt (Ruddiman, 1977). Several recent studies have shown that sediments from the Northeast Atlantic region are exceptionally suitable for investigating

[1] To whom correspondence should be addressed. Fax: 49-431-600-2941. E-mail: jhelmke@geomar.de.

00335-5894/02 $35.00

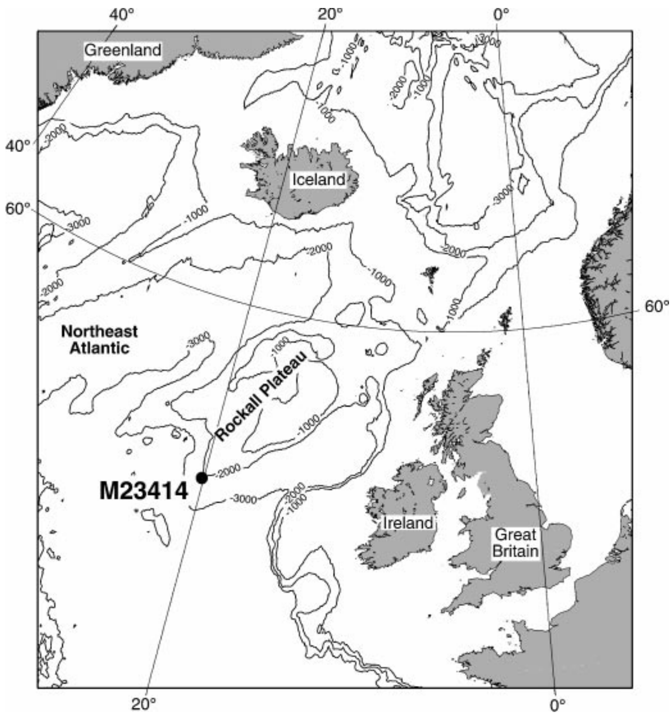

FIG. 1. Geographic position of the core site in the Northeast Atlantic (53°32′N, 20°17′W, 2200 m water depth).

the behavior of glacial and interglacial climate variability on millennial time scales (e.g., Oppo *et al.*, 1998, McManus *et al.*, 1999; Bauch *et al.*, 2000). Sediment-color measurements on the core were carried out at centimeter steps, using a handheld Minolta CM 2002 spectrophotometer. We use lightness L^* and red–green chromaticity a^* of the spherical $L^*a^*b^*$ color space (b^* denotes blue–yellow chromaticity). Precision of the downcore color measurements was investigated using a set of 10 repeated measurements at three spots of the core. The mean standard deviation for these measurements is 0.06 for L^* (range of L^* values between 43.52 and 86.98) and 0.01 for a^* (range of a^* values between -0.52 and 4.19), resulting in typical signal-to-noise ratios of ~500–700. Additionally, the lightness and red–green color variations of separate tracks down the core were measured. The differences are negligible with correlation coefficients (Spearman's rank-order correlation) of $\rho = 0.98$ for lightness ($p < 0.001, n = 469$) and $\rho = 0.93$ for red–green color ($p < 0.001, n = 41$). These results clearly indicate that the spectrophotometer color data faithfully record downcore color fluctuations.

The good agreement between planktic oxygen isotope values (data from Jung, 1996), lightness, and carbonate concentration over the past 250,000 yr indicates that the latter two proxies can be used with confidence to identify the glacial and interglacial periods for the entire record. (Fig. 2a). Due to the good resemblance between the lightness and the SPECMAP oxygen isotope records, ages were assigned to downcore lightness and red–green color data by synchronizing the lightness record to the standard SPECMAP chronology (Imbrie *et al.*, 1984; Martinson *et al.*, 1987), employing constant sedimentation rates between the correlated stratigraphic levels (Fig. 2b). In addition, four accelerator mass spectrometry ^{14}C ages and published ages of six Heinrich events (Sarnthein *et al.*, 2001) were included to refine the age model of the last 60,000 yr. The ^{14}C ages were converted into approximate calendar ages using the software CALIB 4.1.2 (Stuiver *et al.*, 1998) and following Voelker *et al.* (1998). Heinrich events were identified based on the concentration of lithic grains in the size fraction >250 μm (Didié and Bauch, 2000).

This approach assumes that no phase offset exists between ice-volume variations, as recorded by the SPECMAP stack, and changes in $CaCO_3$ concentration, as documented by the lightness record. Although we cannot rule out the possibility that productivity-driven changes in $CaCO_3$ concentration and ice-volume variations occurred asynchronously, possible phase offsets of up to 3000 yr would not alter the main conclusions presented below. Tuning the planktic or benthic oxygen isotope record of site M23414 to the SPECMAP stack is hampered because these data cover only the last 250,000 yr (Jung, 1996). Moreover, both benthic and planktic oxygen isotope data display a shift of ~1.9‰ during the last glacial-to-interglacial transition, which is larger than expected from the ice-volume effect alone (~1.2‰; Chappell *et al.*, 1996). Accordingly, changes in temperature and/or salinity most likely affected both oxygen isotope records (Bauch *et al.*, 2000). Since temperature variations may have led changes in ice-volume (Shackleton, 2000), tuning either of the oxygen isotope series to the SPECMAP chronology would, therefore, not necessarily improve the age model.

LINKING SEDIMENT COLOR TO CLIMATE

Previous studies indicate that red–green color in North Atlantic deep-sea sediments is primarily controlled by the deposition of iron- and manganese-bearing components (Nagao and Nakashima, 1992). For core M23414 it seems most likely that variations in the concentration of red-colored, iron-bearing minerals are responsible for changes in the red–green chromaticity of the sediment. Investigations from sites in the vicinity of M23414 suggest that the deposition of the red-colored mineral hematite in the Northeast Atlantic during the last 40,000 yr is linked to millennial-scale climate variations (Bond and Lotti, 1995; Bond *et al.*, 1997, 1999). These authors proposed that hematite-stained lithic grains stemming from continental red beds were transported via ice rafting to the core sites. X-ray fluorescence (XRF) analysis of samples from M23414 proved that the iron (measured as iron oxide) content of the sediment correlates with the red–green color, i.e., a higher iron content goes along with higher red–green values (Fig. 3). The correlation is significant on the basis of Spearman's rank-order correlation coefficient ($\rho = 0.89$, $p < 0.001$, $n = 10$). Concentrations of specific iron-bearing minerals are too low to be identified using X-ray diffraction (XRD). Since hematite can be identified by XRD down to

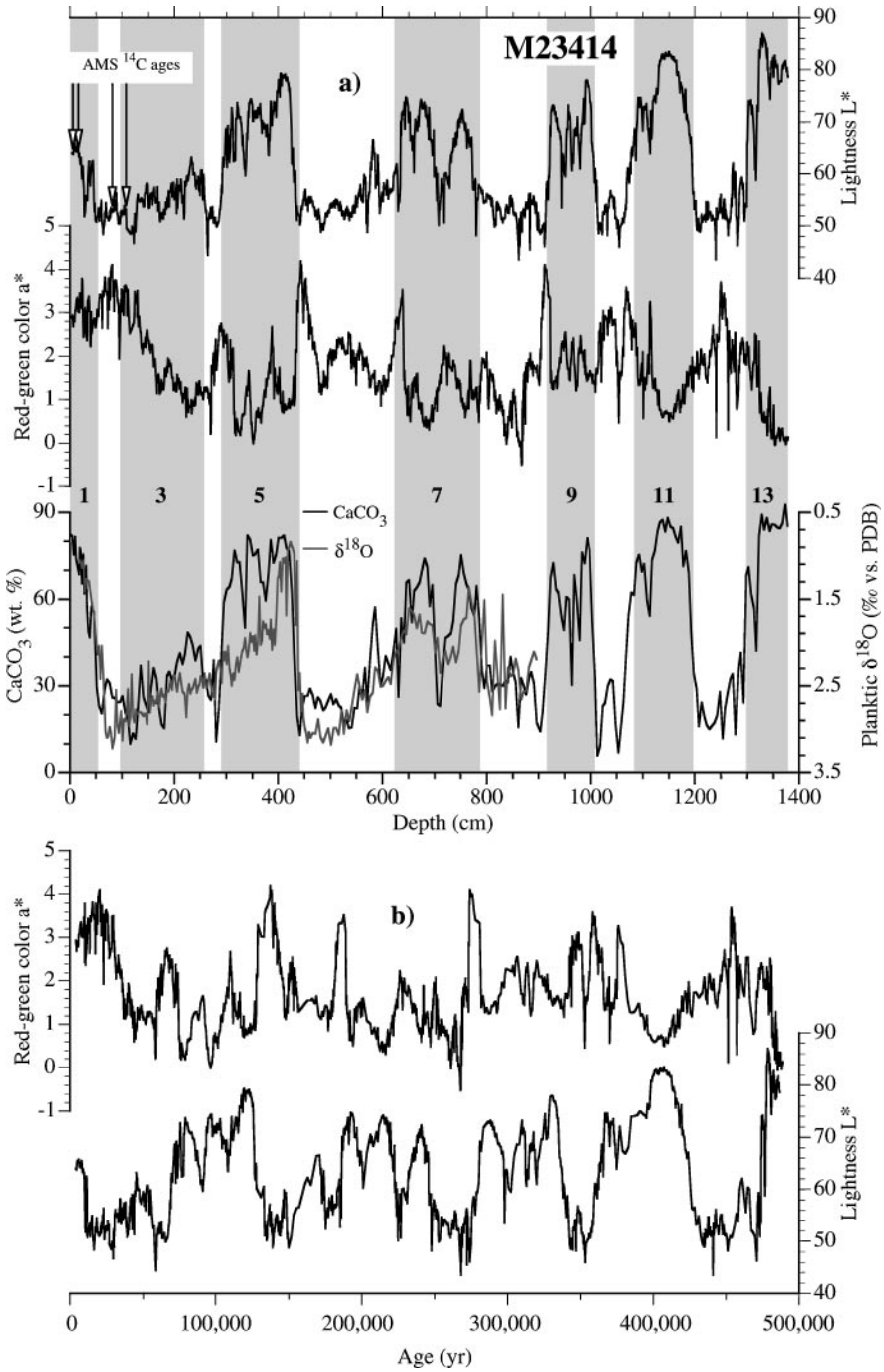

FIG. 2. (a) Downcore records of lightness L^*, red–green chromaticity a^*, and $CaCO_3$ content (weight percentage) from composite core M23414. Oxygen isotope values of the planktic foraminifera *Globigerina bulloides* from M23414-9 (gray line) cover only the upper 900 cm. $CaCO_3$ content and oxygen isotopes were measured at average sample resolutions of 5 cm (Helmke and Bauch, 2001) and 2.5 cm (Jung, 1996), respectively. Arrows mark depth sections with accelerator mass spectrometry (AMS) ^{14}C ages. Odd numbers indicate marine isotope stages for reference and are shaded in gray. (b) Red–green chromaticity a^* (top) and lightness L^* (bottom) *vs* age. The age model is based on the spliced SPECMAP time scale (Imbrie *et al*., 1984; Martinson *et al*., 1987).

concentrations of ∼1% (Deaton and Balsam, 1991) the XRF-derived iron concentrations of up to 7% (Fig. 3) suggest that the red sediment at the study site is composed of several iron oxides, not of hematite only. These findings are further supported by the first-derivative curve of the sediment reflectance spectrum (Fig. 4), a processing method previously used to identify red-colored iron minerals in marine sediments (Barranco *et al*., 1989; Balsam and Deaton, 1991). The presence of hematite leads to a

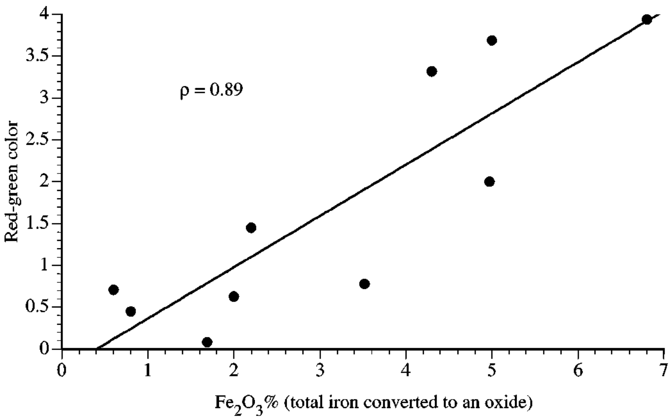

FIG. 3. Correlation of Fe_2O_3 (weight percentage of total iron converted to an oxide) and red–green color for a series of 10 sediment samples from M23414.

single peak at 575 ± 10 nm in the first-derivative curve (for concentrations $>0.1\%$), whereas the primary first-derivative peak of pure goethite occurs at 545 nm (Barranco *et al.*, 1989). Spectra from hydrated oxides are variable and exhibit several peaks at shorter wavelength in the first-derivative curve (Barranco *et al.*, 1989). The first-derivative curve of the reflectance data from M23414 is consistent with such a mixture of several iron oxides showing two peaks, a larger one at 555 nm and a smaller one at 435 nm (Fig. 4b).

A comparison of red–green color and IRD concentration generally reveals good agreement between the records (Fig. 5). In particular the upper parts of the records (Fig. 5b) strongly suggest that changes in red–green color are linked to changes in the concentration of IRD. A somewhat weaker correspondence emerges if the entire time series is considered. This may be

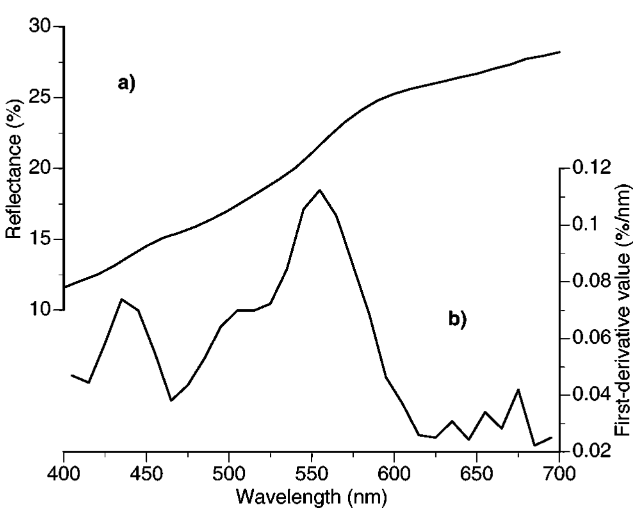

FIG. 4. (a) Average reflectance spectrum of all core sections where red–green chromaticity $a^* \geq 3.5$, i.e., intervals where reddish sediment color is most intensive. (b) First derivative of the reflectance spectrum in (a). The distinct peaks at 555 nm and 435 nm indicate that the red color results from a mixture of hematite and of other iron oxides (cf. Fig. 3 in Balsam and Deaton, 1991).

due to various sources of IRD at the Rockall Plateau during the last 500,000 yr. For example, intervals of IRD input originating primarily from the British–Irish ice sheet, with the Paleozoic red sandstone rocks of the British Isles as a potential source of red-colored IRD components, may lead to a stronger correlation of red–green color and IRD than intervals of major IRD input stemming from other circum–North Atlantic ice sheets. This is in agreement with recent observations in which the IRD pattern and abundance of iron at the northeastern margin of the North Atlantic IRD belt reflect advances and retreats of the British–Irish ice sheet (Richter *et al.*, 2001). However, further possible sources of reddish terrigenous material at the study site are the Proterozoic and Phanerozoic red beds of North America and East Greenland (Bond and Lotti, 1995) as well as iron-rich clay minerals stemming from Iceland.

The correlation of red–green chromaticity and total organic matter is very weak ($\rho = 0.23$, $p < 0.001$, $n = 268$); thus it is unlikely that organic matter should have a strong influence on the red–green color record. An influence of pore-water geochemistry on the red–green color record cannot be ruled out completely. However, oxidation of minerals containing green-colored Fe^{2+} into red-colored minerals containing Fe^{3+} during intervals of low sediment accumulation seems unlikely: A comparison of accumulation rates and red-green color during the last 60,000 yr, for which the time scale is most accurate, indicates that red-green color is not linked to changes in accumulation rate (correlation is not significant: $\rho = -0.05$, $p = 0.911$, $n = 8$).

Hence, we infer that variations in red–green color over the last 500,000 yr are mainly controlled by fluctuations in the input rate of iron-bearing minerals into the sediment, which in turn is linked to climate variations. In contrast, the interpretation of the lightness record is hampered by the fact that sediment lightness is affected by several mechanisms, such as carbonate productivity and preservation, concentrations of organic matter, and IRD, that may even counterbalance each other during a climatic perturbation (Balsam *et al.*, 1999; Bond *et al.*, 1999). To avoid ambiguous interpretations, we therefore restrict the following discussion to the red–green time series.

QUANTIFYING CLIMATE VARIABILITY

The visual alignment of the lightness record to the SPECMAP time scale rests on the identification of congruent patterns in both records. In the SPECMAP time series, the shortest patterns are associated with the precessional cycle of the Earth's orbit, having a periodicity of about 21,000 yr (Imbrie *et al.*, 1984). Since it is possible to identify and align half-precessional cycles in both records, the accuracy of the resulting age model will at least be half the period of the precessional cycle (relative to the SPECMAP chronology). On the other hand, the centimeter-sampled color data have an average resolution of approximately 360 yr (sample resolution ranges between 70 and 2000 yr), making them, in principle, suitable for resolving millennial-scale climate variability. Spectral analysis is commonly employed to

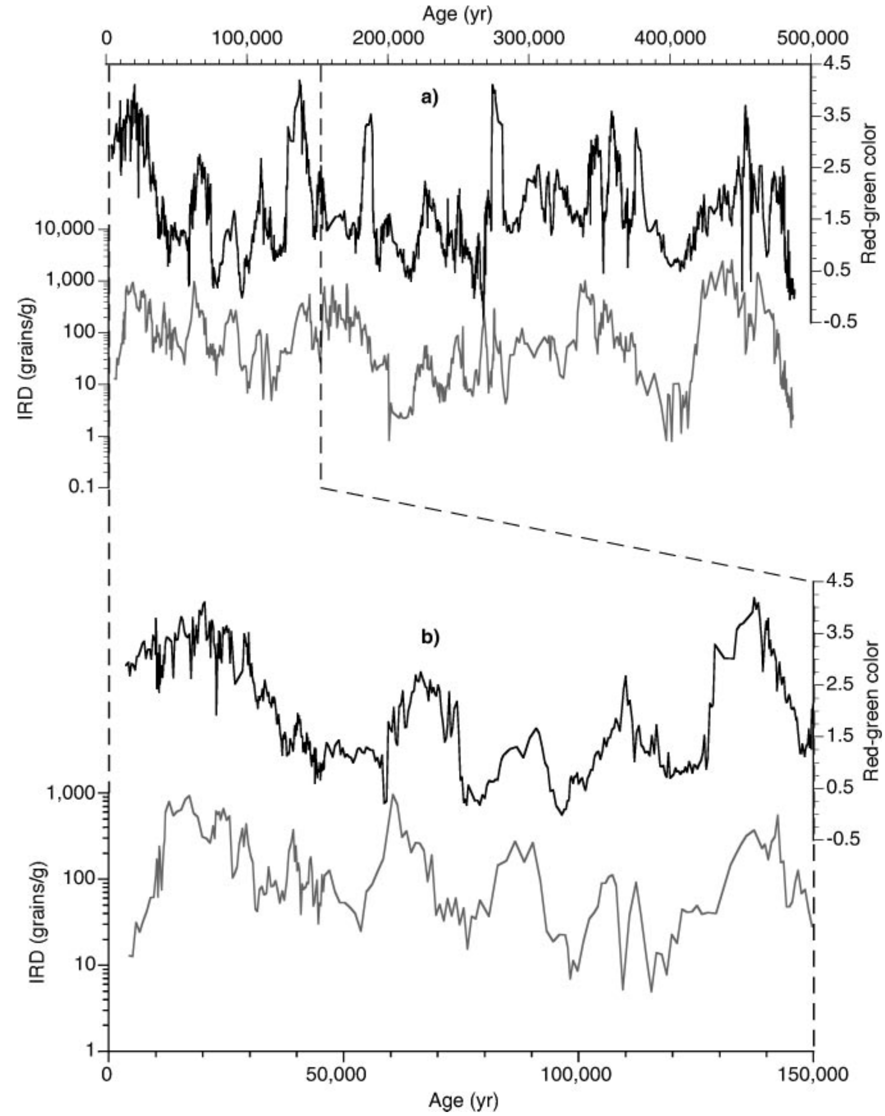

FIG. 5. (a) Records of red–green color and ice-rafted debris concentration (lithic grains per gram) from M23414 vs age. Note logarithmic ordinate scale. (b) Same records as (a) but enlarged for the upper 150,000 yr.

detect and quantify the contribution of millennial-scale variance to the total variance of the series under consideration. However, the uncertainty of the age model makes it unlikely that any distinct spectral peaks in the millennial band, which may have been recorded by the time series, will show up in a spectrum.

Nevertheless, to quantify climate variability in the millennial band, we first filtered the red–green color time series with a high-pass filter (Rybicki and Press, 1995) using a cutoff frequency of $1/12{,}000\ \text{yr}^{-1}$, which is approximately half the precessional period (Fig. 6). The filtered time series thus reflects climate variability from millennial down to multicentennial time scales (limited by the average temporal resolution of the color record). In a second step, the variance of the filtered time series was estimated as a function of time. For this purpose a 8000-yr-wide "sliding window" was moved pointwise along the filtered time series**.** The variance of the filtered data within the window was determined and plotted against the mean age of the data points. (Note that due to the uneven spacing of the time series the number of data points in the window may vary.) Selection of the window width is a compromise between minimizing the uncertainty of the estimated variance (which decreases with a wider window) and maximizing the temporal resolution (which requires a narrow window). The selected width of 8000 yr offers a good compromise between statistical and systematic errors and the results are robust for reasonable choices of the window width; for widths between 6000 and 10,000 yr the results are almost indistinguishable (not shown). Since variance and the area under a spectrum measure the same quantity (Parseval's theorem; Bendat and Piersol, 1986), this approach indirectly estimates spectral power in the entire millennial-to-multicentennial band

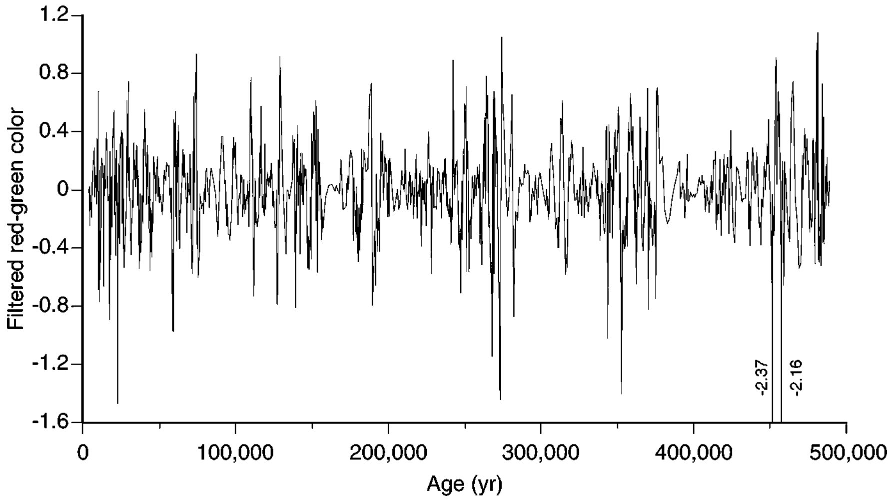

FIG. 6. High-pass-filtered red–green color time series (see Fig. 1b). Cutoff frequency is 1/12,000 yr^{-1}, i.e., approximately half a precessional cycle.

as function of time. Both computational steps were performed on the unevenly spaced time series to prevent any bias in spectral character caused by interpolation to an even sampling interval (Horowitz, 1974; Schulz and Stattegger, 1997).

PATTERNS OF CLIMATE VARIABILITY

Time-dependent variance of the red–green color shows that millennial-scale fluctuations with different amplitudes persisted during the past half a million years (Fig. 7). The comparison of the time-dependent variance of the red–green color record with the SPECMAP oxygen isotope record, which is a proxy for global sea level and therefore continental ice mass (Imbrie *et al*., 1984), reveals that nine variance maxima occurred during time intervals of ice-sheet growth, while three maxima go along with times of ice-sheet decay (Fig. 7). In particular, the variance maxima fall near the end of ice-growth intervals and near the start of ice-decay intervals, rather than at midtransition. Moreover, these variance maxima coincide with times when sea level was 40% of its value during the last glacial maximum, i.e., -50 ± 4 m (Fig. 7), indicating threshold behavior. This agrees with previous studies suggesting that a minimum amount of continental ice is required to sustain prominent climate fluctuations on millennial time scales (Oppo *et al*., 1998; Chapman and Shackleton, 1999; McManus *et al*., 1999; Schulz *et al*., 1999). The range for this threshold results from the uncertainty of sea level at the last glacial maximum (between 121 ± 5 m (Fairbanks, 1989) and 130–135 m (Yokoyama *et al*., 2000)) and is in accordance with the value derived from ice-core data for the last 100,000 yr (Schulz *et al*., 1999). The variance maximum at 315,000 yr is seemingly at odds with this inferred SPECMAP-based threshold. However, according to Berger *et al*. (1996) sea level at this time may have been 18 m lower than indicated by the SPECMAP series, bringing this variance maximum in line with our estimated threshold value. Of the five glacial terminations only Terminations III and II, the glacial-to-interglacial transitions from marine isotope stages 8 to 7, and 6 to 5, respectively, are characterized by variance maxima. Although this suggests different dynamical behavior across glacial-to-interglacial transitions, future studies are needed to confirm this pattern.

Prominent variance minima, indicating low-amplitude millennial-scale climate variability, are generally associated with peak interglaciations (Fig. 7), that is, intervals with small continental ice mass. The two variance minima at 53,000 and 164,000 yr seem to contradict our estimated threshold (Fig. 7**)**. However, radiometrically dated corals (Chappell *et al*., 1996) indicate that sea level at ~50,000 yr was indeed in the range of our threshold. Further investigations are required to test if the same holds true for the relatively warm interval within glacial marine isotope stage 6 at 164,000 yr. During glacial maxima, millennial-scale climate variability is low, although higher than during peak interglaciations, which corroborates the observations of McManus *et al*. (1999) and Schulz *et al*. (1999).

In contrast to findings from the North Atlantic region (Chapman and Shackleton, 1999; McManus *et al*., 1999; Schulz *et al*., 1999; this study) the nonexistence of an ice-volume threshold for high-amplitude millennial-scale climate variability in the subtropical western Atlantic has been recently infered on the basis of a planktic oxygen isotope record, which covers only the interval from 69,000 to 144,000 yr (Oppo *et al*., 2001). However, applying the same signal processing methods as we used to the record from the subtropical Atlantic reveals a variance maximum at approximately 85,000 yr (not shown), which is thus coeval to the occurrence of the first large-amplitude Dansgaard–Oeschger interstadial (DO 21) in the GISP2 ice-core record (Stuiver and Grootes, 2000) and coincides with a brief sea-level drop below our inferred threshold (cf. Fig. 7). Accordingly, the record from the subtropical Atlantic analyzed by Oppo *et al*. (2001) is consistent with the existence of an ice-volume threshold.

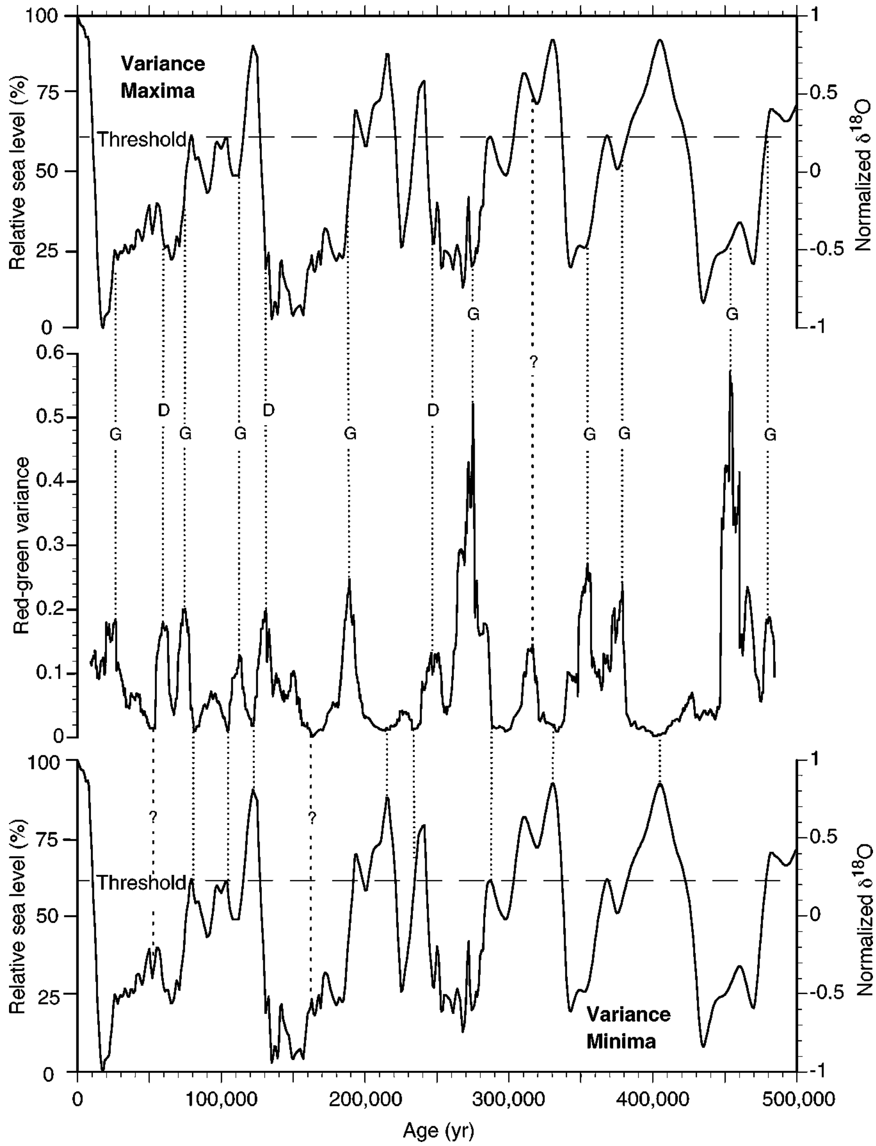

FIG. 7. Ties between millennial-scale variance (center) of the red–green color time series and sea level. Relative sea level is derived from the normalized SPECMAP oxygen isotope record (Imbrie *et al*., 1984; Martinson *et al*., 1987) with 0% corresponding to the last glacial maximum value (for clarity shown twice; top/bottom). Variance maxima coincide with times of either sea-level rise (ice decay; denoted by D) or sea-level drop (ice growth; denoted by G), as indicated by the dotted lines between the two upper records. An exceptional maximum occurs at 315,000 yr (short dashed line), when SPECMAP-derived sea level is probably overestimated (see text for details). Variance minima are tied to times with sea level above a threshold of approximately 40% of the last glacial maximum value (long dashed line), as indicated by the dotted lines between the two lower records. Two apparent exceptions occur at 53,000 and 164,000 yr (short dashed lines), when SPECMAP-derived sea level is probably underestimated (see text for details).

CONCLUSIONS

A red–green color record from Northeast Atlantic deep-sea sediments reveals variations in the amplitude of millennial-scale variability during the past 500,000 yr. Changes in red–green color intensity are probably linked to varying input of reddish terrigenous material by ice rafting, which in turn is closely connected to climate variations on sub-Milankovitch time scales.

Using sea level as proxy for continental ice mass, our results indicate that large-amplitude climate variations are restricted to times when continental ice volume exceeds a threshold, equivalent to sea level at approximately 40% of its value during the last glacial maximum. This value is almost indistinguishable from an earlier estimate, derived for the last 100,000 yr based on ice-core data. It is remarkable and favorable for future modeling studies that a single threshold value apparently controlled the cessation of large-amplitude millennial scale climate variations over the past five glacial-to-interglacial cycles.

Once continental ice mass exceeds the threshold value, maxima of millennial-scale climate variability are tied to times of changes in ice mass. In contrast, relatively stable ice volume during glacial maxima goes along with considerable dampening of climate variability. The inferred relationship between ice volume and "agility" of the climate system to undergo short-term fluctuations seems to hold throughout the past 500,000 yr.

ACKNOWLEDGMENTS

The authors thank W. L. Balsam and W. F. Ruddiman for their thoughtful reviews, which helped to improve the manuscript. The work was supported by the Deutsche Forschungsgemeinschaft (J.H., H.B.) and EU Project "Climate Variability—How Unusual Is the Holocene?" (MS).

REFERENCES

Alley, R. B., Anandakrishnan, S., and Jung, P. (2001). Stochastic resonance in the North Atlantic. *Paleoceanography* **16,** 190–198.

Balsam, W. L., and Deaton, B. C. (1991). Sediment dispersal in the Atlantic Ocean: Evaluation by visible light spectra. *Reviews in Aquatic Sciences* **4,** 411–447.

Balsam, W. L., Deaton, B. C., and Damuth, J. E. (1999). Evaluating optical lightness as a proxy for carbonate content in marine sediment cores. *Marine Geology* **161,** 141–153.

Barranco, F. T., Balsam, W. L., and Deaton, B. C. (1989). Quantative reassessement of brick red lutites: Evidence from reflectance spectrophotometry. *Marine Geology* **89,** 299–314.

Bauch, H. A., Erlenkeuser, H., Jung, S. J. A., and Thiede, J. (2000). Surface and deep water changes in the subpolar North Atlantic during Termination 2 and the last interglaciation. *Paleoceanography* **15,** 76–84.

Bendat, J. L., and Piersol, A. G. (1986). "Random Data." Wiley, New York.

Berger, W. H., Bickert, T., Yasuda, M. K., and Wefer, G. (1996). Reconstruction of atmospheric CO_2 from ice-core data and the deep-sea record of Ontong Java plateau: The Milankovitch chron. *Geologische Rundschau* **85,** 466–495.

Bond, G. C., and Lotti, R. (1995). Iceberg discharges into the North Atlantic on millennial time scales during the last glaciation. *Science* **267,** 1005–1010.

Bond, G. C., Heinrich, H., Broecker, W. S., Labeyrie, L., McManus, J. F., Andrews, J., Huon, S., Jantschik, R., Clasen, S., Simet, C., Tedesco, K., Klas, M., Bonani, G., and Ivy, S. (1992). Evidence for massive discharges of icebergs into the North Atlantic ocean during the last glacial period. *Nature* **360,** 245–249.

Bond, G. C., Showers, W., Cheseby, M., Lotti, R., Almasi, P., deMenocal, P., Priore, P., Cullen, H., Hajdas, I., and Bonani, G. (1997). A pervasive millennial-scale cycle in North Atlantic Holocene and glacial sediments. *Science* **278,** 1257–1266.

Bond, G. C., Showers, W., Elliot, M., Evans, M., Lotti, R., Hajdas, I., Bonani, G., and Johnson, S. (1999). The North Atlantic's 1-2 kyr Climate Rhythm: Relation to Heinrich Events, Dansgaard/Oeschger Cycles and the Little Ice Age. *In* "Mechanisms of Global Climate Change at Millennial Time Scales" (P. U. Clark, R. S. Webb, and L. D. Keigwin, Eds.), pp. 35–58. Geophysical Monograph. Am. Geophys. Union, Washington, DC.

Broecker, W. S., Bond, G. C., and Klas, M. (1990). A salt oscillator in the glacial Atlantic? The concept. *Paleoceanography* **5,** 469–477.

Chapman, M. R., and Shackleton, N. J. (1999). Global ice-volume fluctuations, North Atlantic ice-rafting events, and deep-ocean circulation changes between 130 and 70 ka. *Geology* **27,** 795–798.

Chappell, J., Omura, A., Esat, T., McCulloch, M., Pandolfi, J., Ota, Y., and Pillans, B. (1996). Reconcilation of late Quaternary sea levels derived from coral terraces at Huon Peninsula with deep sea oxygen isotope records. *Earth and Planetary Science Letters* **141,** 227–236.

Cortijo, E., Yiou, P., Labeyrie, L., and Cremer, M. (1995). Sedimentary record of rapid climatic variability in the North Atlantic Ocean during the last glacial cycle. *Paleoceanography* **10,** 911–926.

Dansgaard, W., Johnsen, S. J., Clausen, H. B., Dahl-Jensen, D., Gundestrup, N. S., Hammer, C. U., Hvidberg, C. S., Steffensen, J. P., Sveinbjörnsdottir, A. E., Jouzel, J., and Bond, G. C. (1993). Evidence for general instability of past climate from a 250-kyr-ice-core record. *Nature* **364,** 218–220.

Deaton, B. C., and Balsam, W. L. (1991). Visible spectroscopy—a rapid tool for determining hematite and goethite concentration in geological materials. *Journal of Sedimentary Petrology* **61,** 628–632.

deMenocal, P., Ortiz, J., Guilderson, T., and Sarnthein, M. (2000). Coherent high- and low-latitude climate during the Holocene warm period. *Science* **288,** 2198–2202.

Didié, C., and Bauch, H. A. (2000). Species composition and glacial-interglacial variations in the ostracode fauna of the northeast Atlantic. *Marine Micropaleontology* **40,** 105–129.

Fairbanks, R. G. A. (1989). A 17,000-year glacio-eustatitc sea level record: Influence of glacial melting rates on the Younger Dryas event and deep-ocean circulation. *Nature* **342,** 637–642.

Grootes, P. M., and Stuiver, M. (1997). Oxygen 18/16 variability in Greenland snow and ice with 10^{-3}- to 10^5-year time resolution. *Journal of Geophysical Research* **C102,** 26455–26470.

Helmke, J. P., and Bauch, H. A. (2001). Glacial-interglacial relationship between carbonate components and sediment reflectance in the North Atlantic. *Geo-Marine Letters* **21,** 16–22.

Horowitz, L. L. (1974). The effects of spline interpolation on power spectral density. *IEEE Transactions on Acoustics, Speech, and Signal Procecssing* **22,** 22–27.

Imbrie, J., Hays, J. D., Martinson, D. G., McIntyre, A., Mix, A. C., Morley, J. J., Pisias, N. G., Prell, W. L., and Shackleton, N. J. (1984). The orbital theory of Pleistocene climate: Support from a revised chronology of the marine $\delta^{18}O$ record. *In* "Milankovitch and Climate" (A. L. Berger, J. Imbrie, J. D. Hays, G. Kukla, and B. Saltzman, Eds.), pp. 269–305. Reidel, Dordrecht.

Jung, S. J. A. (1996). Wassermassenaustausch zwischen NE-Atlantik und Nordmeer während der letzten 300.000/80.000 Jahre im Abbild stabiler O- und C-Isotope. *Reports SFB 313* **61,** University of Kiel. [In German]

Keeling, C. D., and Whorf, T. P. (2000). The 1,800-year oceanic tidal cycle: A possible cause of rapid climate change. *Proceedings of the National Academy of Sciences* **97,** 3814–3819.

MacAyeal, D. R. (1993). A low-order model of Heinrich event cycle. *Paleoceanography* **8,** 767–773.

Martinson, D. G., Pisias, N. G., Hays, J. D., Imbrie, J., Moore, T. C., and Shackleton, N. J. (1987). Age dating and the orbital theory of the ice ages: Development of a high-resolution 0 to 300,000-Year chronostratigraphy. *Quaternary Research* **27,** 1–29.

McManus, J. F., Oppo, D. W., and Cullen, J. L. (1999). A 0.5-million-year record of millennial-scale climate variability in the North Atlantic. *Science* **283,** 971–975.

Nagao, S., and Nakashima, S. (1992). The factors controlling vertical color variations of North Atlantic Madeira Abyssal Plain sediments. *Marine Geology* **109,** 83–94.

Oppo, D. W., McManus, J. F., and Cullen, J. L. (1998). Abrupt climate events 500,000 to 340,000 years ago: Evidence from subpolar North Atlantic sediments. *Science* **279,** 1335–1338.

Oppo, D. W., Keigwin, L. D., McManus, J. F., and Cullen, J. L. (2001). Persistent suborbital climate variability in marine isotope stage 5 and Termination II. *Paleoceanography* **16,** 280–292.

Ortiz, J., Mix, A., Harris, S., and O'Connell, S. (1999). Diffuse spectral reflectance as a proxy for percent carbonate content in North Atlantic sediments. *Paleoceanography* **14,** 171–186.

Richter, T. O., Lassen, S., van Weering, T. C. E., and de Haas, H. (2001). Magnetic susceptibility patterns and provenance of ice-rafted material at Feni Drift, Rockall Trough: Implications for the history of the British-Irish ice sheet. *Marine Geology* **173,** 37–54.

Ruddiman, W. F. (1977). Late Quaternary deposition of ice-rafted sand in the subpolar North Atlantic (lat 40° to 65°N). *Geological Society of America Bulletin* **88,** 1813–1821.

Rybicki, G. B., and Press, W. H. (1995). Class of fast methods for processing irregularly sampled otherwise inhomogenous one-dimensonal data. *Physical Review Letters* **74,** 1060–1063.

Sakai, K., and Peltier, W. R. (1997). Dansgaard-Oeschger oscillations in a coupled atmosphere-ocean climate model. *Journal of Climate* **10,** 949–970.

Sarnthein, M., Stattegger, K., Dreger, D., Erlenkeuser, H., Grootes, P. M., Haupt, B., Jung, S. J. A., Kiefer, T., Kuhnt, W., Pflaumann, U., Schäfer-Neth, C., Schulz, H., Schulz, M., Seidov, D., Simstich, J., van Krefveld, S., Vogelsang, E., Voelker, A. H. L., and Weinelt, M. (2001). Fundamental modes and abrupt changes in North Atlantic circulation and climate over the last 60 ky—Concepts, reconstruction, and numerical modelling. *In* "The Northern North Atlantic: A Changing Environment" (P. Schäfer, W. Ritzrau, M. Schlüter, and J. Thiede, Eds.), pp. 365–410. Springer-Verlag, Heidelberg.

Schulz, M. The tempo of climate change during Dansgaard-Oeschger interstadials and its potential to affect the manifestation of the 1470-year climate cycle. *Geological Research Letters*, in press.

Schulz, M., and Stattegger, K. (1997). Spectrum: Spectral analysis of unevenly spaced paleoclimatic time series. *Computer and Geosciences* **23,** 929–945.

Schulz, M., Berger, W. H., Sarnthein, M., and Grootes, P. M. (1999). Amplitude variations of 1470-year climate oscillations during the last 100,000 years linked to fluctuations of continental ice mass. *Geophysical Research Letters* **26,** 3385–3388.

Shackleton, N. J. (2000). The 100,000-year ice-age cycle identified and found to lag temperature, carbon dioxide, and orbital eccentricity. *Science* **289,** 1897–1902.

Stuiver, M., and Grootes, P. M. (2000). GISP2 oxygen isotope ratios. *Quaternary Research* **53,** 277–284.

Stuiver, M., Reimer, P. J., Bard, E., Beck, J. W., Burr, G. S., Hughen, K. A., Kromer, B., McCormac, G., van der Pflicht, J., and Spurk, M. (1998). INTCAL98 radiocarbon age calibration, 24,000-0 cal BP. *In* "INTCAL 98: Calibration Issue" (M. Stuiver and J. van der Pflicht, Eds.), *Radiocarbon* **40,** 1041–1083.

van Geel, B., Raspopov, O. M., Renssen, H., van der Pflicht, J., Dergachev, V. A., and Meijer, H. A. J. (1999). The role of solar forcing upon climate change. *Quaternary Science Reviews* **18,** 331–338.

van Kreveld, S. A., Sarnthein, M., Erlenkeuser, H., Grootes, P. M., Jung, S. J. A., Nadeau, M. J., Pflaumann, U., and Voelker, A. H. L. (2000). Potential links between surging ice sheets, circulation changes and the Dansgaard-Oeschger cycles in the Irminger Sea. *Paleoceanography* **15,** 425–442.

Voelker, A. H. L., Sarnthein, M., Grootes, P. M., Erlenkeuser, H., Laj, C., Mazaud, A., Nadeau, M.-J., and Schleicer, M. (1998). Correlation of marine ^{14}C ages from the Nordic seas with the GISP2 isotope record: Implications for radiocarbon calibration beyond 25 ka BP. *Radiocarbon* **40,** 517–534.

Winton, M. (1993). Deep coupling oscillations of the oceanic thermohaline circulation. *In* "Ice in the Climate System" (W. R. Peltier, Ed.), pp. 417–432. NATO ASI Series. Springer-Verlag, Berlin.

Yokoyama, Y., Lambeck, K., De Deckker, P., Johnston, P., and Fifield, L. K. (2000). Timing of the last glacial maximum from observed sea-level minima. *Nature* **406,** 713–716.